Experimental and Numerical Investigation of Heat Conduction in Porous Media

Hana Salati

Submitted to the
Institute of Graduate Studies and Research
In partial fulfilment of the requirements for the Degree of

Master of Science
in
Mechanical Engineering

Eastern Mediterranean University
January 2014
Gazimağusa, North Cyprus

Approval of the Institute of Graduate Studies and Research

Prof. Dr. Elvan Yılmaz
Director

I certify that this thesis satisfies the requirements as a thesis for the degree of Master of Science in Mechanical Engineering.

Prof. Dr. Uğur Atikol
Chair, Department of Mechanical Engineering

We certify that we have read this thesis and that in our opinion it is fully adequate in scope and quality as a thesis for the degree of Master of Science in Mechanical Engineering.

Prof. Dr. Hikmet Ş. Aybar
Supervisor

Examining Committee

1. Prof. Dr. Hikmet Ş. Aybar _____

2. Prof. Dr. Fuat Egelioğlu _____

3. Assoc. Prof. Dr. Hasan Hacışevki _____

ABSTRACT

Heat transfer in porous media has recently become an important subject in mechanical engineering. This study presents experimental and numerical investigations of the effective thermal conductivity in porous media. A porous sample (pumice stone) has been used in experimental investigations. Bottom and upper parts of the sample were cooled and heated using heat exchanger and the water thermal bath. The interior temperatures of four different locations of the sample were measured at various times. Then, the effective thermal conductivity of the material was calculated. The experiment was modeled and simulated and the governing equation was numerically solved using finite difference method. The obtained value of effective thermal conductivity of material was very close to the values have been found in literatures.

Keywords: Porous Media, Thermal conductivity, Effective Thermal Conductivity

ÖZ

Gözenekli ortamda ısı transferi son zamanlarda daha önemli olmuş bir konudur. Bu çalışmada, gözenekli ortamda etkili termal iletkenlik, deneysel ve sayısal inceleme sunulmuştur. Deneysel kısımda, gözenekli numune (ponza taşı) kullanılmıştır. Alt ve üst numune ısı değiştiricisi ve su banyosu tarafından ısıtıdu ve soğutuldu. Numunenin dört farklı yerde iç sıcaklıkları farklı zamanlarda ölçülür. Daha sonra, malzemenin etkin ısı iletkenliği hesapladı. Deney modellenmiş ve simulasyon. yapılmıştır. denklemler, sonlu farklar yöntemi kullanılarak sayısal olarak çözülmüştür. FORTRAN kullanılarak bilgisayar kodu geliştirilmiştir. Malzemenin etkin ısı iletkenliği, literatürde bulunan değerlere çok yakındır.

Anahtar kelimeler: Gözenekli medya, Isı iletkenlik, Etkin termal iletkenlik

To My Family

ACKNOWLEDGMENT

First, I would like to thank Prof. Dr. Hikmet Ş. Aybar who has supported me through my thesis and for his excellent guidance and knowledge. Without his invaluable supervision, it would have been impossible for me to complete this work.

I would also like to thank Mr. Mehdi Moghadasi for his considerable help and encouragement. Also I would like to show my gratitude to all of my friends who helped me through this study.

Finally, I would like to thank my family for their unconditional support, both financially and emotionally during the last two and half years.

TABLE OF CONTENTS

LIST OF TABLES

LIST OF FIGURES

LIST OF SYMBOLS

A	Area (m^2)
C_p	Specific heat of water (J /kg.℃)
k	Thermal conductivity (W/m.℃)
k_s	Thermal conductivity of solid (W/m.℃)
k_f	Thermal conductivity of fluid (W/m.℃)
$\dot{m}$	Mass flow rate (kg/s)
$\dot{\mathbf{Q}}$	Energy (J)
T	Temperature (℃)
$\Delta\mathbf{T}$	Temperature difference (℃)
V	Volume (m^3)

Greek Symbols

α	Thermal diffusivity (m^2/ s)
ε	Porosity of sample
ρ	Density (kg/m^3)

Subscript

c	Cold
F	Fluid
h	hot
S	Solid

Chapter 1

INTRODUCTION

A porous material contains pores. It has two phases; solid and fluid phases and its skeleton is a frame or a matrix.

Heat transfer is a fundamental subject in many problems, which contributes to transport of flow through a porous medium [1]. Many researchers have studied the heat conduction in porous media. They used several analytical models to predict thermal behavior of porous materials. Numerical methods such as finite difference [2] and finite element [3] methods usually have been used for prediction of effective thermal conductivity in porous materials.

Effective thermal conductivity plays an important role in many engineering applications, such as chemical engineering and soil sciences [4]. Thermal conductivity in porous media depends on various elements such as properties of phases and microstructure parameters [5]. Heat conduction in porous media is macroscopically described as averaging the microscopic heat transfer over a representative elementary volume [6]. Computation of heat conduction in porous materials is related to the micro-geometry structure of pore. Usually a local thermal equilibrium is assumed for steady heat conduction between two phases in porous material. Therefore, the processes of macroscopic heat transfer in fluid and solid phases can be lumped into a single heat conduction equation [7].

1.1 Objective of the Study

This study was performed experimentally and numerically to obtain the thermal conductivity and the temperature distribution within a porous sample (pumice stone). The experimental analysis was carried out on a steady state and the sample was simulated by using the energy equation. The governing equations have been solved by means of finite difference method. The properties of the sample such as porosity and density were measured experimentally. The aim of this study is to compute experimentally and numerically the effective thermal conductivity of porous material.

1.2 Thesis Organization

The previous researches are summarized in chapter 2. Chapter 3 demonstrates the development of the experiment and introduces instruments and devices, which have been used in this research. Chapter 4 briefly describes discretization and energy equations in porous media using finite difference method. Figures and tables extracted from numerical and experimental results have been presented in chapter 5. Chapter 6 provides a conclusion of the research presented in this thesis.

Chapter 2

LITERATURE REVIEW

The application of heat conduction in porous media has been involved in many engineering applications [7]. Many researchers have done experimental and numerical investigations on the heat conduction of different materials.

Aichlmayr and Kulacki [8] used semi-infinite cylinder with constant heat flux at boundary to measure effective thermal conductivity. Based on mathematical solution and ohm‘law, Ganji [1] applied the transient technique to measure the effective thermal conductivity.

Thermal conductivity of porous materials is influenced by characteristics of materials such as geometry of pore structure, micro structural parameters and properties of phases [9, 10].

Researchers used suspended platinum hot film for measuring thermal conductivity based on one-dimensional analysis [11].

Jannot et al. [12] developed a method to measure thermal conductivity of very low density insulating materials. They utilized three layer systems to find input and output temperature. The results demonstrated that the sensitivity to thermal diffusivity and thermal conductivity were changed by changing the sample thickness.

They concluded that it is very difficult to measure thermal diffusivity for very low density insulating materials [12].

Bernasconi et al.[13] proposed a study about measuring thermal conductivity and heat capacity of the silica aerogels. The aim of their study was to develop a model in order to overcome the problems of the low density and serious effect on thermal characteristic of a sample.

Fourie and DU Plessis [14, 15] performed a study on measuring heat transfer in porous media using two equation models; equilibrium and non-equilibrium temperature distribution. Fourie and Plessis [14, 15] proved that two equation models can become into one-equation model when there is a thermal equilibrium between two phases.

Vitro et al. [16] experimentally investigated the thermal conductivity coefficient and thermal diffusivity of three materials ; Bronze, Sand and Cotton with different properties. They showed that thermal conductivity coefficient and thermal diffusivity depend on thermal conductivity of a solid matrix.

Measuring heat conduction fundamentally depends on micro-geometry structure of porous media, Lv et al. [6] found a direct relation between effective thermal conductivity and increasing porosity. Lv et al. [6] proved that in a porous media, thermal conductivity is related to micro-geometry structures, volume fraction of fluid, and liquid phases.

Vosteen and Schellschmidt [17] mesaured thermal conductivity of different type of rocks at ambient temperature. Vosteen and Schellschmidt [17] showed that the thermal conductivity of rocks decreases with temperature and specific heat capacity of rocks increases with temperature.

Thermal conductivity measurement of anisotropic two-phase media were introduced by Akbari et al. [18]. They showed that the effective thermal conductivity was correlated as a tensor to the rectangular Cartesian transformation group. They showed that the obtained diagonal effective thermal conductivity tensor was the result of the elliptical inclusion symmetry.

Different effective techniques are also developed, which allow us to calculate the effective thermal conductivity of a porous media [19]. Regression equations can be used to predict the thermal conductivity [20]. The test conducted by Usowics et al on terrestrial soils and snow showed that regression equations are dependent on porosity, penetration resistance, and content of sand for different soils.

Nait-Ali et al [21] proposed the evaluation of the effect of humidity on the thermal conductivity of porous media by changing the water content. Nait-Ali et al [21] used Zirconia powder as their sample and studied the heat conduction in a dry porous media and a liquid porous media. Their experiments showed that the thermal conductivity increases with the water content.

Saito and de Lemos [22] applied two-energy equation model for conduction and convection heat transfer in porous media. Saito and de Lemos [22] studied the effect of Nusselt number on porosity of fluid and solid phases.

Chapter 3

EXPERIMENTAL INVESTIGATION

3.1 Experimental Setup

The experimental setup is shown in Fig.3.1. Two water thermal baths, two heat exchangers, data acquisition system, and PC were used for the experiment. Four holes have been drilled in the sample for measuring temperatures. Two heat exchangers were used. One of the heat exchanger was used for heating and the other was used for cooling and then they were connected to the water thermal bath with flexible pipes. The sample, heat exchangers, and flexible pipes were insulated. Thermocouples were used to measure temperatures. Some of the thermocouples were placed in the sample and the others were inserted in inlet and outlet of the hot/cold water thermal bath.

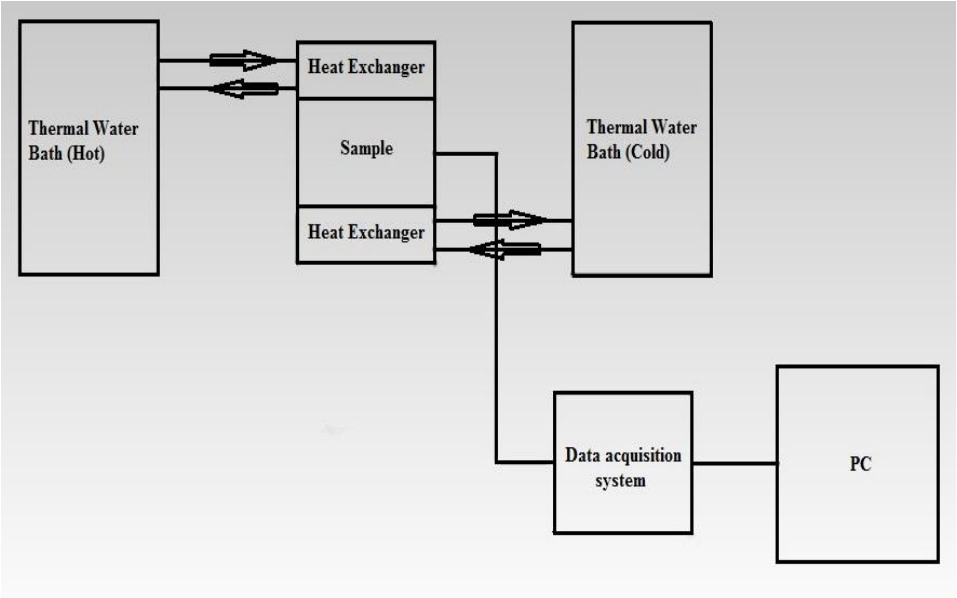

Figure 3.1**.** Schematic diagram of the experimental apparatus

3.1.1 Sample

Pumice was selected as the porous sample for this study. After determining the Porosity, the pumice was cut into the specified dimension. The dimension of pumice was measured by caliper. The dimension and proportion of the sample are presented in table 3.1.

Table 3.1**.** Pumice Dimension and properties

Length	12cm
Width	5.1cm
Thickness	8cm
Porosity	0.313
Mass	0.293 kg
ρ	598.44 kg/m^3
C_p	1000 J /kg.℃

Figure 3.2 shows the locations of four holes drilled in pumice.

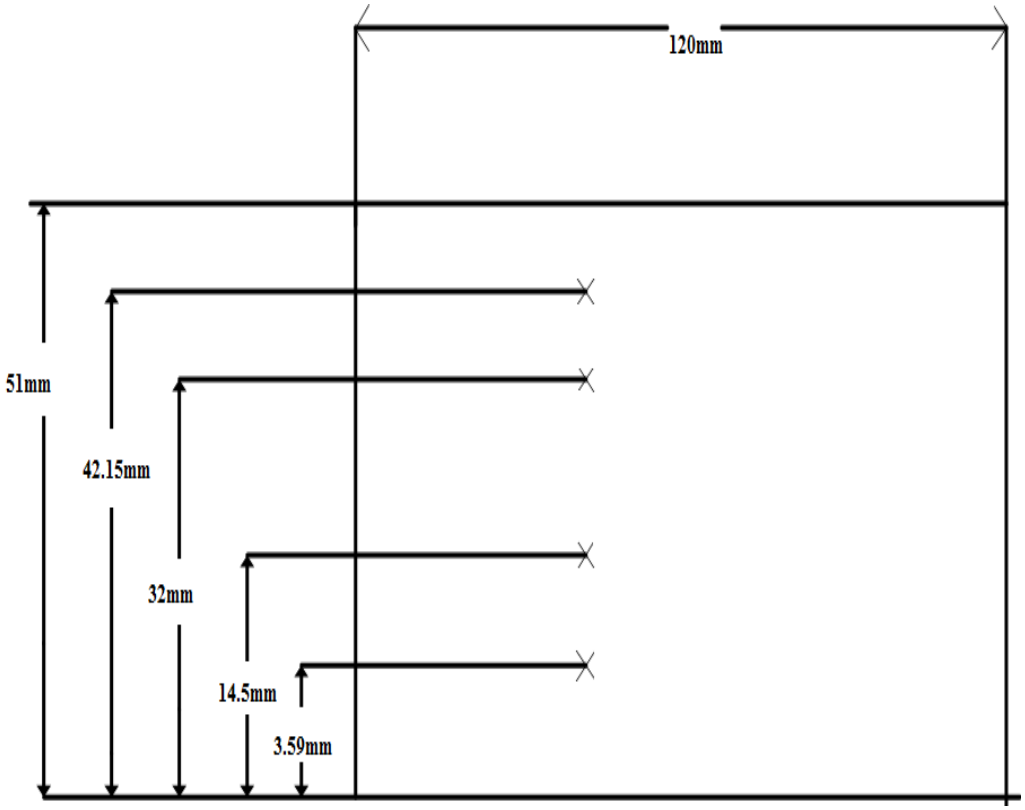

Figure 3.2. Locations of holes and sample dimension (millimeter)

3.1.2 Heat Exchanger

Heat exchanger is a device used for efficient heat transfer. Brass material was used as the heat exchanger in this study.

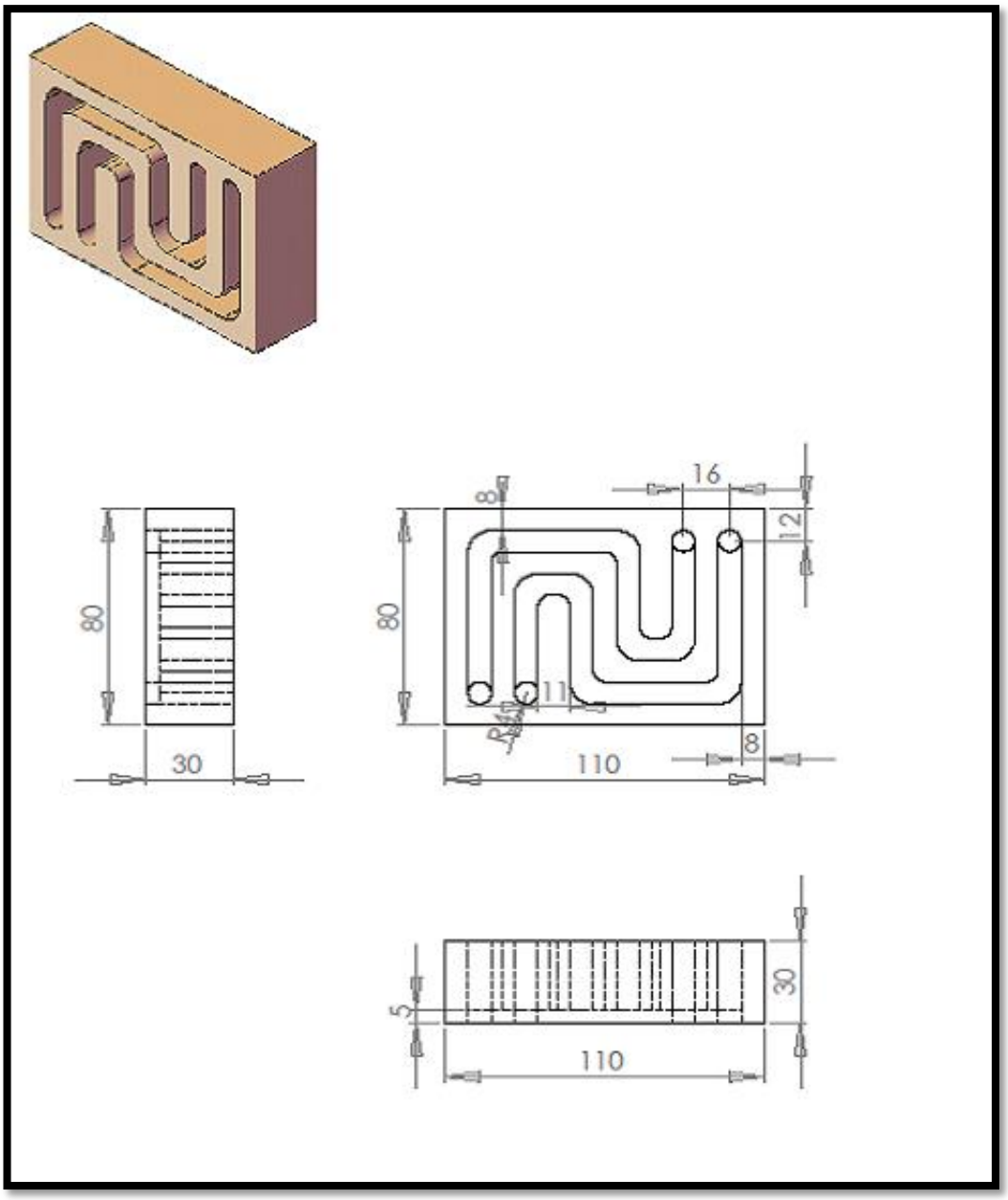

Figure 3.3. Schematic Design of the Heat Exchanger

3.1.3 Expanded Polystyrene and Flexible Pipe

Expanded polystyrene is a good insulation. In this study, the sample and the heat exchangers were insulated by expanded polystyrene. Four flexible pipes were used to connect heat exchanger to water thermal bath.

3.1.4 Water Thermal Bath

The water thermal bath is consists of two parts; heated water and cooled water. Before starting the experiment, water was poured into devices. Water thermal bath was first operated to reach the steady temperature. Steady temperature was achieved after 7.66 hour. The flexible pipes were connected from the heat exchangers to water thermal bath.

3.1.5 Thermocouple

Thermocouple is a temperature-measuring device consisting of two conductors that connected at one spot for creating a small voltage. Four thermocouples were placed in holes of the sample. The other parts connected to data acquisition system with positive and negative poles. The other thermocouples placed in input and output parts of heated and cooled water. The k type thermocouple was used in this study. The thermocouple error is ±0.5 ℃.

3.1.6 Data Acquisition System

Data Acquisition System is a device that converts resulting sample into digital numeric values which is connected to computer**.** Acquisition of this system based on gathering signals which can measure real physical conditions and convert them into digital and/or numeric values that can be processed by a computer. Data acquisition systems (or DAQ systems) typically can convert analog waves into digital values in order to process them. The DAQ device used in this experiment is an Omega device of model OM-DAQ-USB-2400 series. It has 16 single channels or 8 differential channels at higher accuracy. It measures the temperature with the accuracy of ±0.01 ℃.

3.1.7 Flow Meter

A flow meter is an instrument used to measure linear, nonlinear, mass or volumetric flow rate of a liquid or a gas, which is connected to the water thermal bath. In this study, the model number of flow meter is lzt. The flow rate is 4 liters per minute.

3.2 Experimental Procedure

As it is shown in Fig.3.1, the cavity including heat exchangers and sample is connected to the water thermal bath. The upper part of heat exchanger is connected to hot water thermal bath by two flexible pipes in which one of them is inlet hot water and other one is the outlet hot water. The lower part of heat exchanger is connected to cold water thermal bath same as the upper one. In this study, eight thermocouples were used. Four thermocouples connect the sample to the data acquisition system and the other four thermocouples were placed in inlet and outlet parts of hot/cold water and the data acquisition system.

The data acquisition system is joined to the computer, and then the water thermal bath was turned on. After turning on, the set of the temperatures including eight columns were appeared on the computer. After 7.6 hour steady temperatures reached and temperatures of the inlet and outlet hot/cold as well as internal temperatures of the sample were shown in the computer.

Figure 3.4**.** The Cavity and Flexible pipes

Chapter 4

SIMULATION OF EXPERIMENT

4.1 Mathematical Modeling

In this study, the governing equations are the unsteady heat conduction which is parabolic Partial differential equation (equation 4.1).

$$\frac{\partial T}{\partial t} = \alpha \frac{\partial^2 T}{\partial X^2} \tag{4.1}$$

Where:

$$\alpha = \left(\frac{k}{\rho Cp}\right) \tag{4.2}$$

Where:

k is thermal conductivity, ρ is density and Cp is specific heat capacity.

The properties of the sample (pumice) were discussed in chapter 3. Energy equation used for porous media is different from energy equation applied for other materials. By writing codes in FORTRAN programming, temperature distribution in the sample was calculated and then they were compared to the experimental results. Conductivity was unknown in the experimental results, so it was calculated by given temperatures and energy equation.

The equation 4.1 is the unsteady state energy equation in porous media.

The formulation of porosity in porous media is:

$$\varepsilon = \frac{Vf}{V} \tag{4.3}$$

$$(C_p) = (1-\varepsilon)(\rho C_p)_s + \varepsilon(\rho C_p)_f \tag{4.4}$$

$$k = \frac{kf\,[(2kf+ks)-2(1-\varepsilon)(kf-ks)]}{2kf+ks+(1-\varepsilon)(kf-ks)} \tag{4.5}$$

Where: ε is porosity, k_f is thermal conductivity of fluid and k_s is the thermal Conductivity of solid. V_f is the volume of the fluid and V is the volume of the sample.

4.2 Numerical Solution

In this study, finite difference method has been used for numerical investigations. The finite difference equation was written for all grids points. The equations were converted to the matrix form. For solving parabolic equations, there are some methods such as explicit and implicit methods.

Explicit method involves three models:

1. Richardson method
2. The Dufort-Frankel method
3. The Forward time/central space (FTCS) method

Implicit method includes two methods:

1. The Leasonen method
2. The Crank-Nicolson

First, heat conduction equation was descretize for one-dimensional system (eq.4.1). In this method, the general form of formulation is the following equation:

$$a_i^n T_{i-1}^{n+1} + b_i^n T_i^{n+1} + c_i^n T_{i+1}^{n+1} = D_i^n \tag{4.6}$$

Crank-Nicolson method was chosen over other methods for computing those coefficients because of its higher accuracy.

Following equations are the coefficients obtained from implicit method.

$$a_i = \frac{-\alpha \Delta t}{2(\Delta x)^2}$$

$$b_i = \frac{\alpha \Delta t}{(\Delta x)^2} + 1 \qquad (4.7)$$

$$c_i = \frac{-\alpha \Delta t}{2(\Delta x)^2}$$

$$D_i = \frac{\alpha \Delta t}{(\Delta x)^2}\left[-T_i^n + \frac{T_{i+1}^n + T_{i-1}^n}{2}\right] + T_i^n$$

Where: α is thermal diffusivity, Δt is time difference, Δx is distance, T_i^n is the Temperature at point i and at time n, T_{i+1}^n is the temperature at point i+1 and at time n, T_{i-1}^n is the temperature at point i+1 and time n.

General form for two dimensional systems is:

$$a_{i,j}T^{n+1}_{i-1,j} + b_{i,j}T^{n+1}_{i,j} + c_{i,j}T^{n+1}_{i-1,j} + e_{i,j}T^{n+1}_{i,j-1} + f_{i,j}T^{n+1}_{i,j+1} = D^n_{i,j} \qquad (4.8)$$

This numerical study was performed to evaluate and check the accuracy of experimental results. Finite difference method was applied to numerically evaluate and check the accuracy of experimental results.

Grids were defined to find acceptable temperature distribution. By aid of writing codes in Microsoft Visual Studio 2010 (FORTRAN), temperature distribution has been reached. The matrix form is [101×101] with 101 rows and 101 columns. Temperatures were obtained in 10404 nodes. In FORTRAN code, GAUSS-SEIDEL method has been used to solve the matrix.

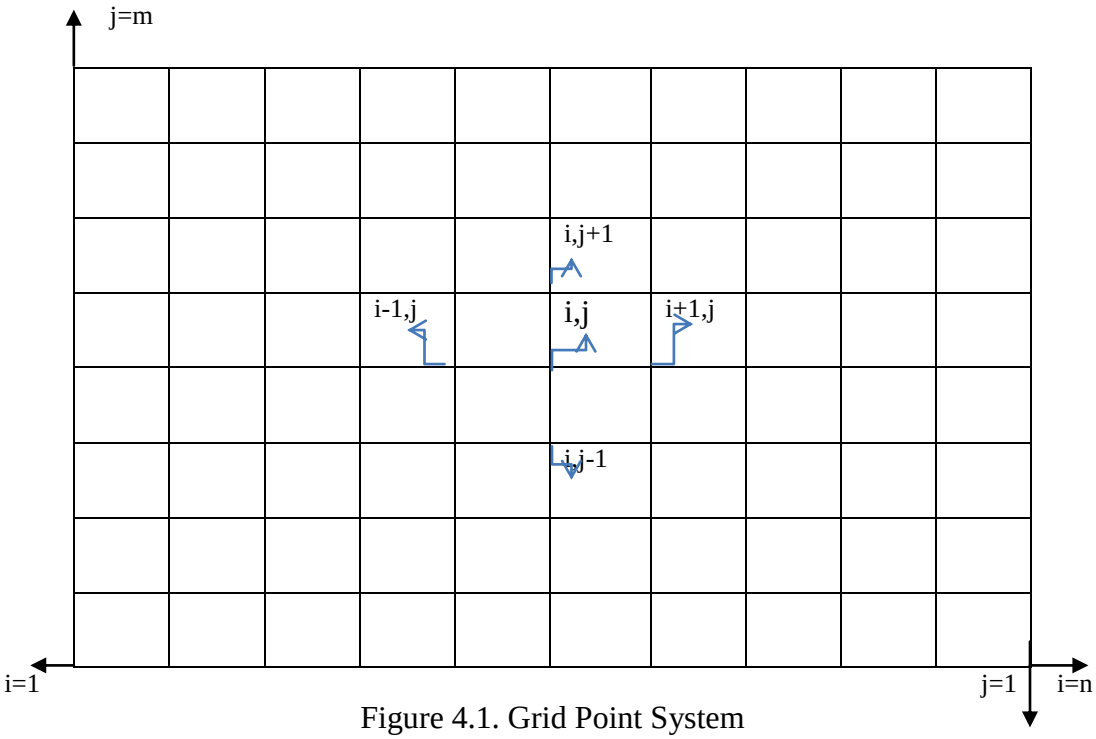

Figure 4.1. Grid Point System

There were two iterations in this numerical calculation. One of the iteration was used in the solver part and another one was used in the solver and the residual parts. The amount of iterations for each part is respectively: 20 and 1000. Figure 4.2 shows the boundary conditions.

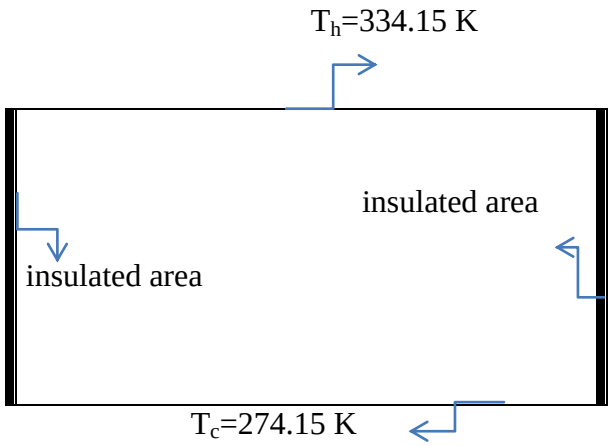

Figure 4.2. Boundary Condition Definitions

Western and eastern boundaries were insulated. It means that temperatures at those boundaries were equal to the temperatures of near boundary cells.

$$\frac{\partial T}{\partial x} = 0 \tag{4.9}$$

According to Eq.4.8 and Fig.4.1, following equations were obtained.

$$T(1,j) = T(2,j)$$
$$T(n,j) = T(n-1,j) \tag{4.10}$$

Conditions of the northern and southern boundaries were clear because of the presence of hot and cold temperatures in those locations. L_x is length.

$$T(x, 0) = T_c$$

$$T(x, L_y) = T_h$$

Where: T_h is the hot temperature, T_c is the cold temperature and L_y is width.

Residual is another important factor which should be defined. In this study, the accuracy of residual is 10^{-8}.

Chapter 5

RESULTS AND DISCUSSIONS

This chapter represents the experimental and numerical results. In the experimental study, different temperatures were obtained for various times.

As it is shown in Figs.5.1 to 5.5, temperatures of the inlet/outlet of hot and cold water and temperatures of the internal part of sample are achieved.

Figure 5.5 shows temperatures at different locations. There are four lines which were reached to steady state at different points.

Table 5.1. Average Temperatures

	Tave
Inlet hot water temperature	61.79 ℃
Outlet hot water temperature	61.85 ℃
Inlet cold water temperature	1.34 ℃
Outlet cold water temperature	1.35 ℃
Temperature in cavity (0.00359 meter from origin)	55.09 ℃
Temperature in cavity (0.0145 meter from origin)	44.26 ℃
Temperature in cavity (0.032 meter from origin)	22.30 ℃
Temperature in cavity(0.04215 meter from origin)	11.77 ℃

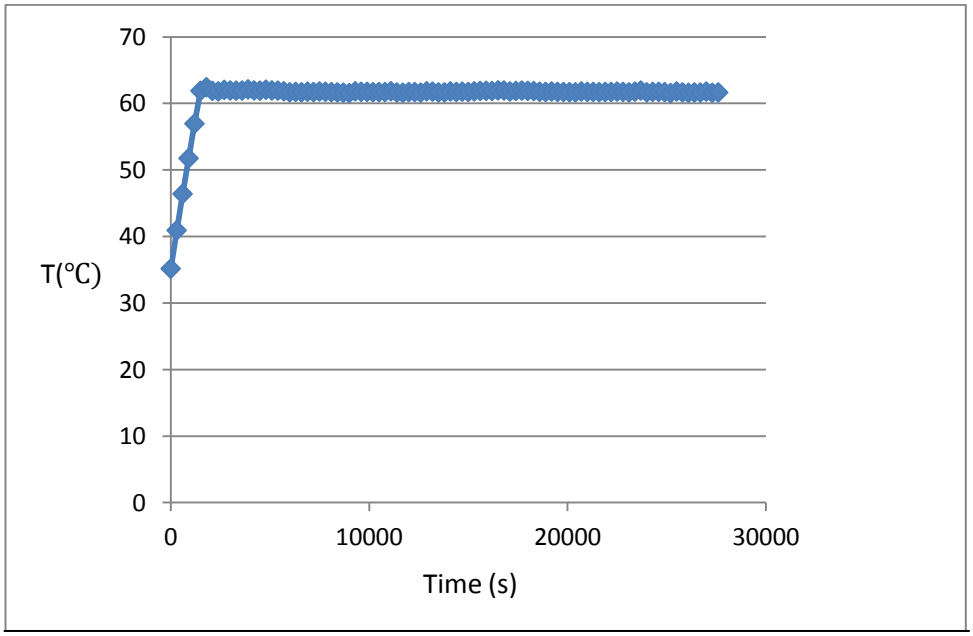

Figure 5.1. Temperature distribution of Inlet hot water at various times

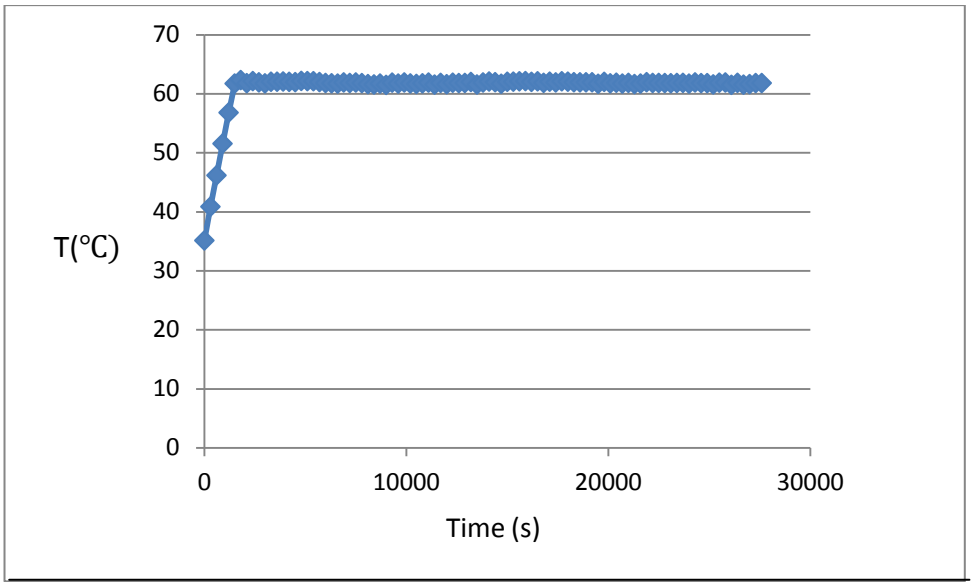

Figure 5.2. Temperature distribution of outlet hot water at various times

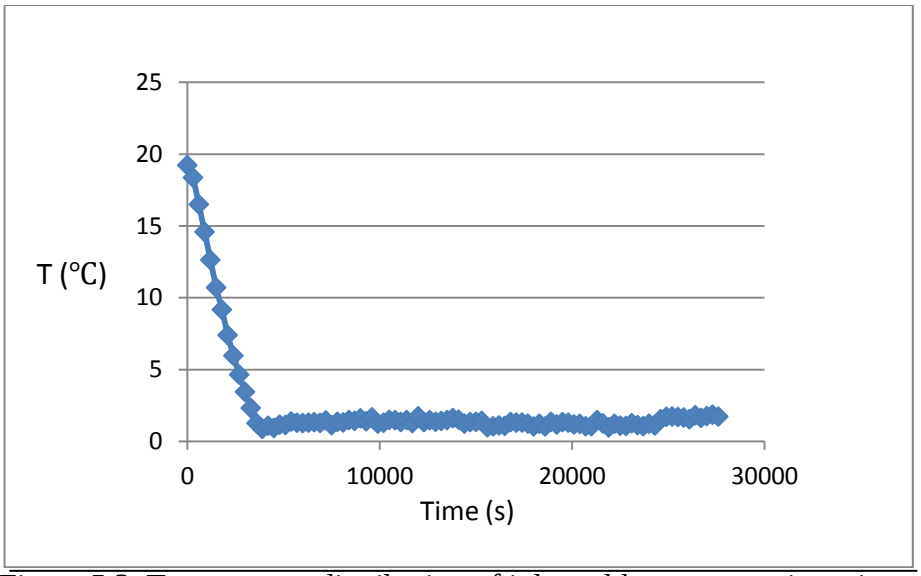

Figure 5.3. Temperature distribution of inlet cold water at various times

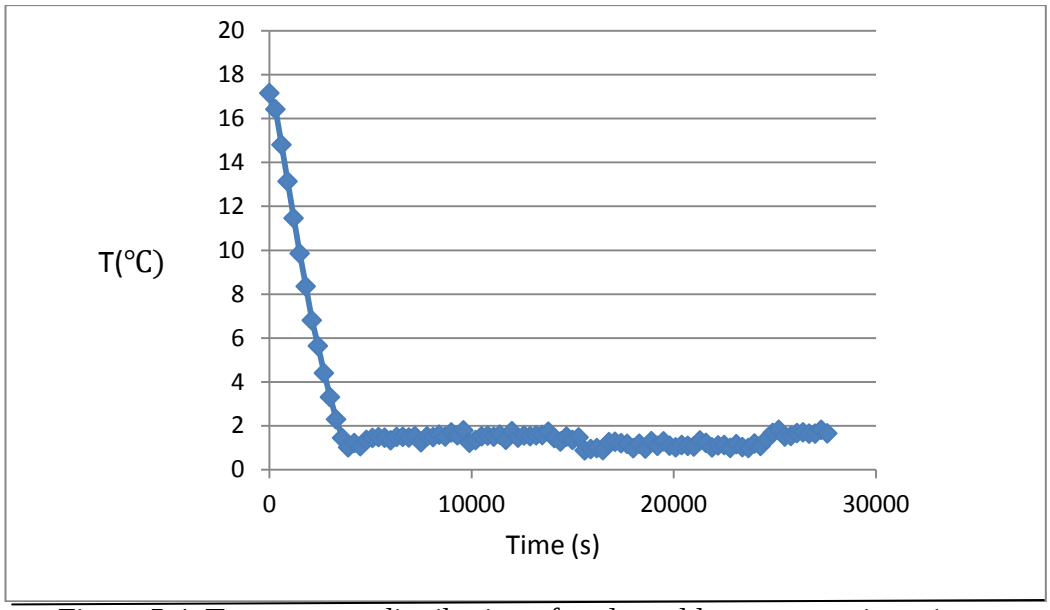

Figure 5.4. Temperature distribution of outlet cold water at various times

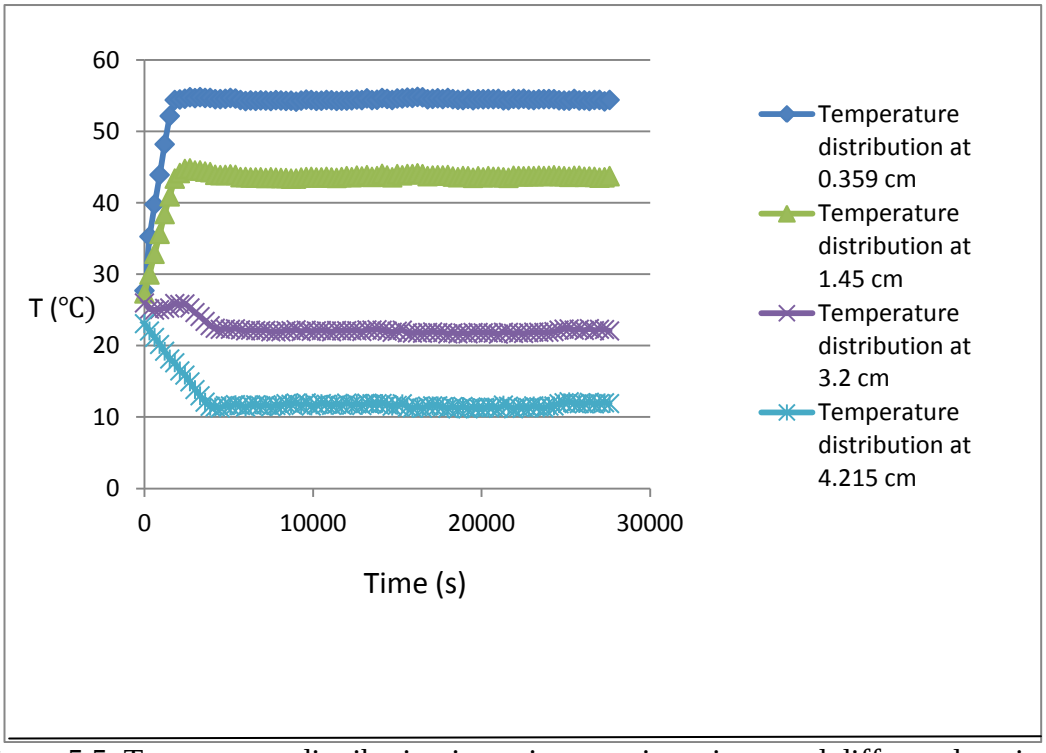

Figure 5.5. Temperature distribution in cavity at various times and different locations

Temperature distribution in cavity between experimental and numerical studies was compared to each other.

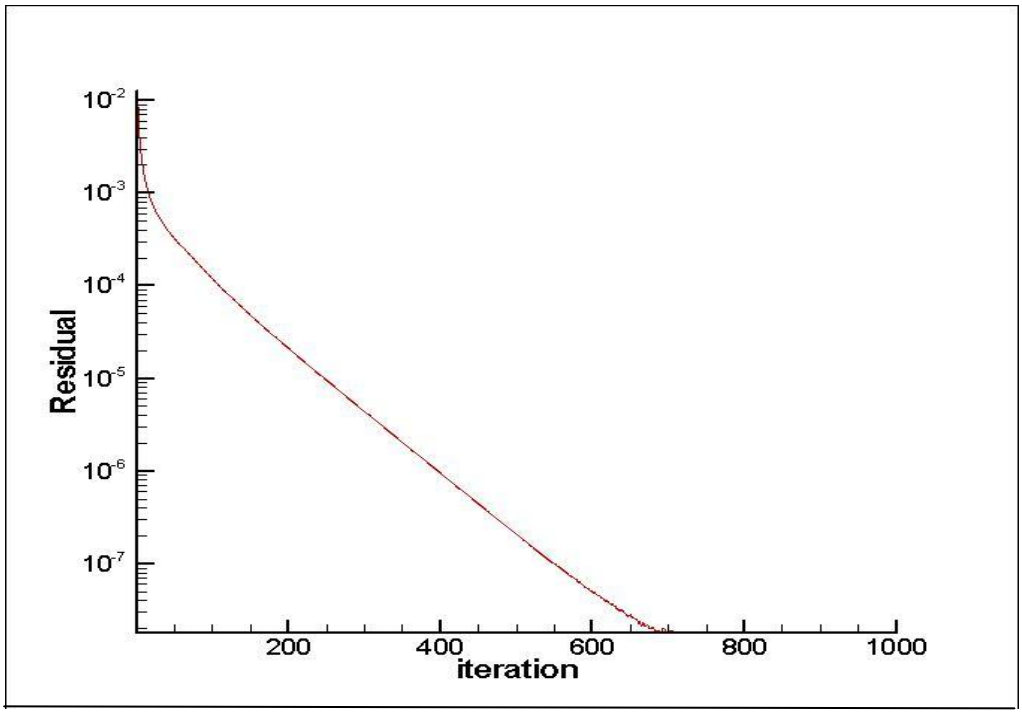

Figure 5.6. Residual graph

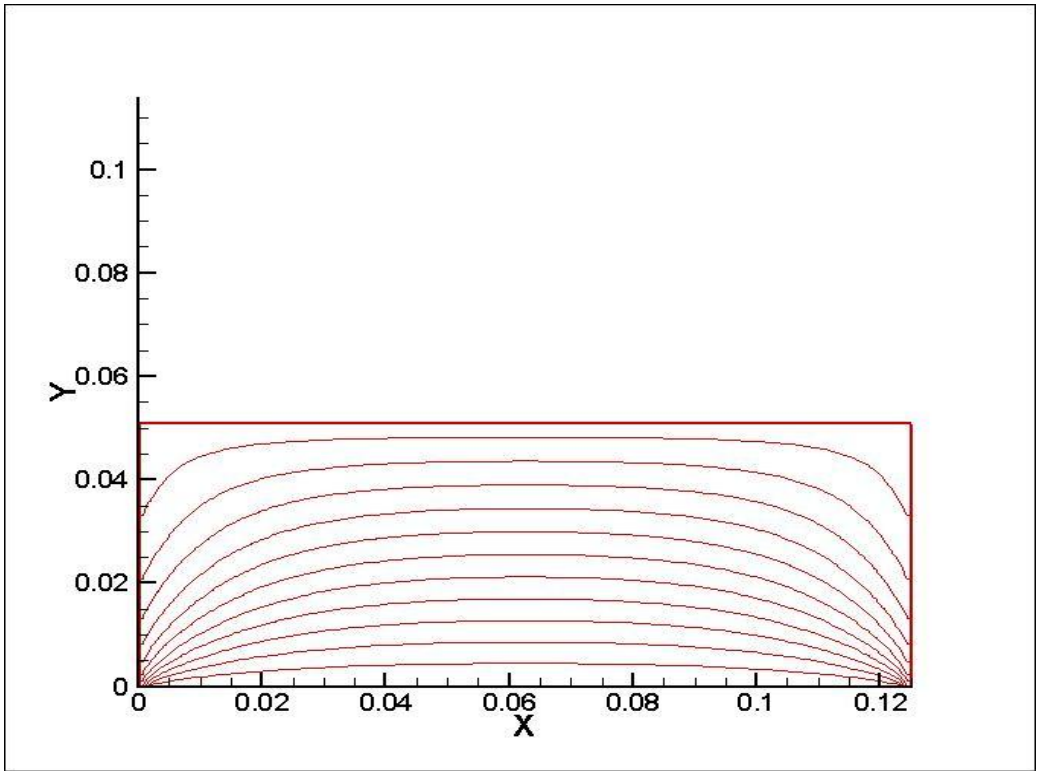

Figure 5.7. Temperature distribution in numerical investigation

Figure 13 shows the residual graph with 1000 iteration. The residual value remains constant at the iteration of 731 and the value is about1.8×10^{-8}.

Figure 5.7 shows the temperature distribution calculated by FORTRAN programming. Eastern and western boundaries were insulated and the temperatures of the northern and southern boundaries are 59.782℃ and 1.3462℃, respectively. These two temperatures were obtained from experimental investigations. This graph was drawn by Tecplot 360.

As it is represented in Fig.5.8, the slope of the graph is equal to $\frac{dT}{dx}$. There is a subtle difference between numerical and experimental results. In the experimental study, factors such as isolation, humidity, and the errors of devices may affect results.

In the numerical investigations, if boundary conditions change then the results would be close to each other.

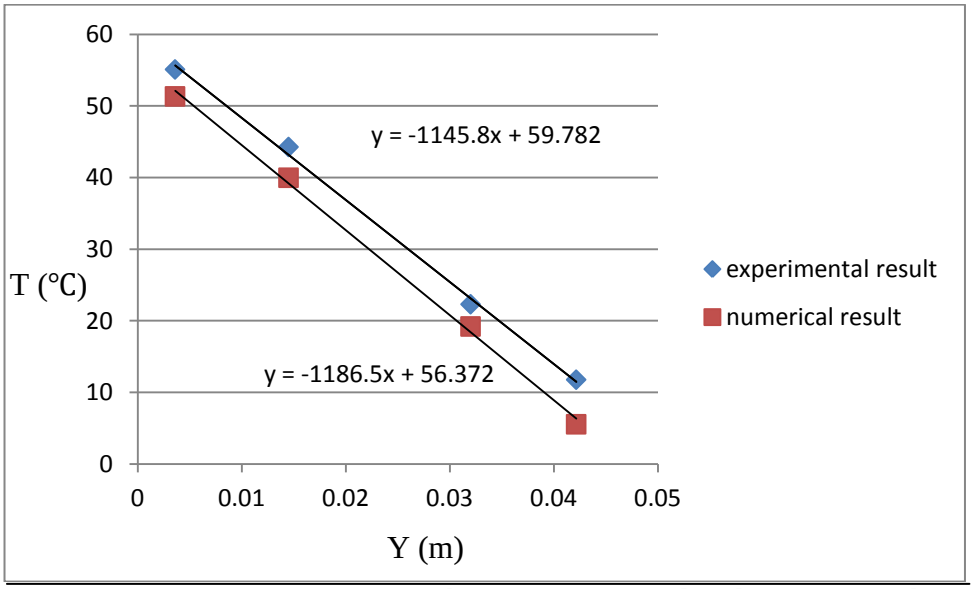

Figure 5.8. Temperature comparisons between numerical and experimental results

Thermal conductivity of the sample was obtained as:

$$\dot{m}C_p\Delta T_c = kA\frac{dT}{dX} \quad (5.1)$$

Where:

C_p: Specific heat capacity of water = 4175 J/kg℃

ṁ: mass flow rate= 4 litre/min

ΔT_c = Average temperature difference of cold water (outlet and inlet) =0.012438 ℃

A: sample area= 0.010625 m²

$\frac{dT}{dX}$= 1145.8

$$k=\frac{\dot{m}Cp\Delta Tc}{A\frac{dT}{dX}} = 0.28 \text{ W/m.K}$$

The acceptable amount of thermal conductivity is between 0.13-0.3 [23] depends on density. It is notable that there are some errors which made the calculated thermal conductivity being a little higher than the acceptable value. In addition, there are other factors such as heat losses and the degree of humidity that affect the obtained results. Because of the geographical situation of North Cyprus, humidity can alter the results. In this study, a lot of attempts have been made in order to decrease those errors. For example, upper cavity was heated and lower cavity was cooled.

According to energy equation, inlet energy is equal to outlet energy.

$\dot{Q}_h$=inlet energy

$\dot{Q}_c$=outlet energy

Where:

ΔT_h=Average temperature difference of hot water (outlet and inlet) =0.06038℃

$\dot{Q}_h = \dot{m}C_p \Delta T_h$ = (0.066) (4175) (0.06038) =16.63 J

$\dot{Q}_c = \dot{m}C_p\Delta T_c$ = (0.066)(4175)(0.012438) = 3.42 J

$\dot{Q}_h$-$\dot{Q}_c$ =13.21 J

There is 13.21 J heat losses in the experimental investigation.

5.1 Error Analysis

In this part, the error of equations, thermal conductivity, and instruments such as dimension of the sample were analyzed. The error of the devices in all experimental researches is inevitable; however, some of them can be neglected.

$\Delta X = 0.125 - 0.12 = 0.005$ m

$\Delta Y = 0.051 - 0.05 = 0.001$ m

$\Delta Z = 0.085 - 0.08 = 0.005$ m

Where:

ΔX is the error of length, ΔY is the error of width and ΔZ is the error of thickness.

A=sample area = 0.0051*0.0085=0.010625 m²

$\Delta A =$ Area error = $0.010625 * \sqrt{(\frac{0.005}{0.125})^2 + (\frac{0.005}{0.085})^2} = 0.000755$ m²

$\dot{m}$ = mass flow rate= 4 lit/min

$\Delta \dot{m} =$ mass flow rate error $= 0.02$ lt/min

$\Delta T =$ data acquisition error $= 0.00019$

k = thermal conductivity (w/m.k) $= \frac{Cp}{\frac{dT}{dX}} \times \frac{\dot{m}\Delta T}{A}$

G = $\dot{m}\Delta T$ = 0.00083

$\Delta G =$ amont of error $= 0.00083 \times \sqrt{\left(\frac{0.02}{0.066}\right)^2 + (\frac{0.00019}{0.012438})^2} = 0.00025$

$\Delta \dot{Q} =$ energy error $= 0.00025 * 4175 = 1.04$ J

$F = A \times \frac{dT}{dX}$

$\Delta F = \Delta A * 1145.8$ = 0.000755 *1145.8 =0.86

$k = \frac{\dot{Q}}{A \times \frac{dT}{dX}} = 0.28$ W/m.K

Thermal conductivity error $= \Delta k = 0.28 \times \sqrt{\left(\frac{1.04}{3.42}\right)^2 + \left(\frac{0.86}{12.17}\right)^2} = 0.086$ W/m.K

Δk= 8.66 %

Chapter 6

CONCLUSION

This study has been done experimentally and numerically parts. Thermal conductivity of pumice was found and numerical and experimental results were compared. Air was used in porous material as the fluid. In the experimental part, steady state has been assumed and then the temperature distribution in cavity was found for different times. Using these results, thermal conductivity was obtained and used for the numerical investigations. Numerical analysis was done using FORTRAN programming. The temperature distribution was calculated in 10404 nodes.

According to the experimental analysis, thermal conductivity is about 0.28 (W/m.℃) which shows a subtle difference from the acceptable value. Some factors affect the procedures such as humidity and devices errors. Because of the high humidity in North Cyprus, the sample was heated from the upper part and the bottom part was cooled. Instruments errors may influence the obtained results. Comparison the numerical graphs and the experimental parts show subtle differences. Figure 5.6 and figure 5.7 represent the temperature distribution in different location of sample (this sentence should be in the result section not conclusion). Thermal conductivity error is about 8.6% ($k = 0.28 \pm 0.08$). Overall, these results are almost close to each other.

REFERENCES

[1] Ganji, E.m.L.a.D.D., Heat transfer in porous media, University of Washington-Milwaukee, Noshirvani Technical University of Babol

[2] Havis, C.R., G.P. Peterson, and L.S. Fletcher, Predicting the thermal conductivity and temperature distribution in aligned fiber composites. Journal of thermophysics and heat transfer, 1989. 3(4): p. 416-422.

[3] Bakker, K., Using the finite element method to compute the influence of complex porosity and inclusion structures on the thermal and electrical conductivity. International Journal of Heat and Mass Transfer, 1997. 40(15): p. 3503-3511.

[4] Kou, J., et al., The effective thermal conductivity of porous media based on statistical self-similarity. Physics Letters, Section A: General, Atomic and Solid State Physics, 2009. 374(1): p. 62-65.

[5] Bouguerra, A., Prediction of effective thermal conductivity of moist wood concrete. Journal of Physics D: Applied Physics, 1999. 32(12): p. 1407-1414.

[6] Lv, Y.G., X.L. Huai, and W.W. Wang, Study on the effect of micro geometric structure on heat conduction in porous media subjected to pulse laser. Chemical Engineering Science, 2006. 61(17): p. 5717-5725.

[7] Hsu, C.T., *A* closur*e* model for transient heat conduction in porous media. Journal of Heat Transfer, 1999. 121(3): p. 733-739.

[8] Aichlmayr, H.T. and F.A. Kulacki, A transient technique for measuring the effective thermal conductivity of saturated porous media with a constant boundary heat flux. Journal of Heat Transfer, 2006. 128(11): p. 1217-1220.

[9] Zumbrunnen, D.A., R. Viskanta, and F.P. Incropera, Heat transfer through porous solids with complex internal geometries. International Journal of Heat and Mass Transfer, 1986. 29(2): p. 275-284.

[10] Prakouras, A.G., et al., Thermal conductivity of heterogeneous mixtures. International Journal of Heat and Mass Transfer, 1978. 21(8): p. 1157-1166.

[11] Takahashi, K., et al., Measurement of the thermal conductivity of nanodeposited material. International Journal of Thermophysics, 2009. 30(6): p. 1864-1874.

[12] Jannot, Y., A. Degiovanni, and G. Payet, Thermal conductivity measurement of insulating materials with a three layers device. International Journal of Heat and Mass Transfer, 2009. 52(5-6): p. 1105-1111.

[13] Bernasconi, A., et al., Dynamic technique for measurement of the thermal conductivity and the specific heat: Application to silica aerogels. Review of Scientific Instruments, 1990. 61(9): p. 2420-2426.

[14] Fourie, J.G. and J.P. Du Plessis, A two-equation model for heat conduction in porous media. Transport in Porous Media, 2003. 53(2): p. 163-174.

[15] Fourie, J.G. and J.P. Du Plessis, A two-equation model for heat conduction in porous media. Transport in Porous Media, 2003. 53(2): p. 145-161.

[16] Virto, L., et al., Heating of saturated porous media in practice: Several causes of local thermal non-equilibrium. International Journal of Heat and Mass Transfer, 2009. 52(23-24): p. 5412-5422.

[17] Vosteen, H.D. and R. Schellschmidt, Influence of temperature on thermal conductivity, thermal capacity and thermal diffusivity for different types of rock. Physics and Chemistry of the Earth, 2003. 28(9-11): p. 499-509.

[18] Akbari, A., M. Akbari, and R.J. Hill, Effective thermal conductivity of two-dimensional anisotropic two-phase media. International Journal of Heat and Mass Transfer, 2013. 63: p. 41-50.

[19] Gruescu, C., et al., Effective thermal conductivity of partially saturated porous rocks. International Journal of Solids and Structures, 2007. 44(3-4): p. 811-833.

[20] Usowicz, B., J. Lipiec, and J.B. Usowicz, Thermal conductivity in relation to porosity and hardness of terrestrial porous media. Planetary and Space Science, 2008. 56(3-4): p. 438-447.

[21] Nait-Ali, B., et al., Effect of humidity on the thermal conductivity of porous zirconia ceramics. Journal of the European Ceramic Society, 2013. 33(13-14): p. 2565-2571.

[22] Saito, M.B. and M.J.S. de Lemos, Laminar heat transfer in a porous channel simulated with a two-energy equation model. International Communications in Heat and Mass Transfer, 2009. 36(10): p. 1002-1007.

[23] Al-Jabri, K.S., et al., Concrete blocks for thermal insulation in hot climate. Cement and Concrete Research, 2005. 35(8): p. 1472-1479.

APPENDICES

Appendix A: Raw Data

Table A.1. Temperature measurement in Experiment

Start Time				
Elapsed Time	AN1D	AN2D	AN3D	AN4D
Seconds	C	C	C	C
0	35.186663	35.130770	27.712282	27.327620
300	40.942740	40.860250	35.278654	29.981790
600	46.424690	46.165270	39.779430	32.876250
900	51.775353	51.540470	43.910139	35.668500
1200	56.979224	56.798730	48.196253	38.437850
1500	61.912213	61.720230	52.155668	40.913760
1800	62.450589	62.309150	54.393670	43.398220
2100	61.912767	61.783460	54.469835	44.175190
2400	61.829287	62.134130	54.572387	44.737680
2700	62.057149	61.923930	54.783383	44.821100
3000	61.966182	61.746580	54.656728	44.525650
3300	61.939489	62.028910	54.797216	44.535600
3600	61.958711	62.034060	54.680113	44.375480
3900	62.133268	62.070000	54.683251	44.295810
4200	61.968522	62.008640	54.509109	43.927700
4500	61.936269	61.962150	54.514062	43.877520
4800	62.087098	62.166070	54.559757	43.910060
5100	61.963455	62.131660	54.679506	43.981940
5400	61.950485	62.119230	54.602824	43.907070
5700	61.852118	61.975700	54.392383	43.601120
6000	61.691815	61.817070	54.242877	43.614510

Start Time				
Elapsed Time	AN5D	AN6D	AN7D	AN8D
Seconds	C	C	C	C
0	25.988130	23.086050	19.226530	17.160030
300	25.121840	22.060970	18.367590	16.422270
600	24.973150	21.159670	16.501340	14.805800
900	25.062030	20.171830	14.579850	13.138710
1200	25.231450	19.224550	12.630250	11.462750
1500	25.284940	18.142110	10.708950	9.853830
1800	25.910850	17.612650	9.167880	8.354544
2100	25.777280	16.471580	7.395171	6.808700
2400	25.859330	15.881070	5.960148	5.642504
2700	25.293090	14.939650	4.643236	4.405416
3000	24.640670	13.858190	3.445974	3.309848
3300	24.079760	12.991310	2.316421	2.296400
3600	23.403350	12.096820	1.263827	1.450093
3900	22.806610	11.512160	0.866653	1.021909
4200	22.443990	11.432730	1.082120	1.217192
4500	22.290570	11.283410	0.928754	1.074075
4800	22.331570	11.626140	1.160497	1.359578
5100	22.299570	11.576150	1.138176	1.450081
5400	22.367320	11.752700	1.377041	1.487121
5700	22.219620	11.612210	1.293976	1.460166
6000	22.081040	11.413420	1.269649	1.342501

Start Time				
Elapsed Time	AN1D	AN2D	AN3D	AN4D
Seconds	C	C	C	C
6300	61.753751	61.766110	54.335533	43.551530
6600	61.702119	61.711870	54.272104	43.546500
6900	61.789331	61.911950	54.343076	43.570420
7200	61.730439	61.815090	54.314585	43.478310
7500	61.814607	61.901670	54.252782	43.576860
7800	61.774092	61.797060	54.378883	43.514930
8100	61.718377	61.626790	54.328159	43.480860
8400	61.673910	61.566600	54.263501	43.460210
8700	61.627950	61.715810	54.300121	43.388520
9000	61.574957	61.488320	54.159008	43.394610
9300	61.846746	61.878150	54.312145	43.537670
9600	61.764714	61.715910	54.447094	43.598570
9900	61.756679	61.905650	54.386747	43.633370
10200	61.718659	61.736880	54.271043	43.547250
10500	61.726146	61.652550	54.299402	43.560090
10800	61.729057	61.761860	54.401361	43.638680
11100	61.852701	61.886090	54.358709	43.547030
11400	61.667670	61.543710	54.270192	43.491180
11700	61.623657	61.830140	54.308760	43.598260
12000	61.723895	61.607250	54.315433	43.732530
12300	61.730607	61.860000	54.355362	43.588150
12600	61.645625	61.800020	54.464807	43.812160
12900	61.839012	61.821990	54.382681	43.689420
13200	61.795586	61.984550	54.629155	43.871150
13500	61.676895	61.557740	54.379466	43.630850

Start Time				
Elapsed Time	AN5D	AN6D	AN7D	AN8D
Seconds	C	C	C	C
6300	22.177620	11.722970	1.299409	1.495212
6600	22.118650	11.727240	1.330650	1.500330
6900	22.102690	11.576110	1.282840	1.469085
7200	22.145090	11.726860	1.449164	1.533722
7500	21.952500	11.446690	1.121105	1.252509
7800	21.948630	11.631150	1.357179	1.520968
8100	21.963130	11.575440	1.310996	1.487936
8400	22.106580	11.891960	1.479327	1.598021
8700	22.113500	11.793460	1.424310	1.513257
9000	22.226960	11.975280	1.601561	1.698325
9300	21.983060	11.645590	1.391148	1.570652
9600	22.160550	11.996060	1.663492	1.795656
9900	22.014770	11.559420	1.230722	1.229224
10200	22.082510	11.709930	1.289165	1.350351
10500	22.127700	11.901370	1.489899	1.525204
10800	22.062830	11.797210	1.474640	1.554947
11100	21.955420	11.653290	1.341416	1.506319
11400	22.136240	11.780780	1.476817	1.599512
11700	22.063560	11.664700	1.268582	1.362995
12000	22.106340	11.966960	1.735762	1.758376
12300	22.094480	11.683300	1.335163	1.462265
12600	22.102000	11.861720	1.469401	1.562417
12900	21.987610	11.625960	1.359428	1.530006
13200	22.207330	11.952160	1.415841	1.570694
13500	22.190520	11.871420	1.475067	1.583262

Start Time				
Elapsed Time	AN1D	AN2D	AN3D	AN4D
Seconds	C	C	C	C
13800	61.676895	61.899510	54.428924	43.738520
14100	61.821033	62.065430	54.671485	44.054000
14400	61.743615	61.952420	54.547691	43.829250
14700	61.792542	61.686070	54.394610	43.576940
15000	61.750515	62.021280	54.612538	44.015020
15300	61.837312	62.039670	54.621651	43.852070
15600	61.891743	62.099850	54.723459	44.027710
15900	61.913201	62.134260	54.688786	44.018770
16200	61.892103	62.005740	54.825683	44.133790
16500	61.977311	62.098540	54.772634	44.012220
16800	61.965835	61.838130	54.500296	43.739750
17100	61.820639	62.038890	54.549073	43.815430
17400	61.897813	61.912890	54.637325	43.857860
17700	61.952942	62.105210	54.525744	43.829630
18000	61.906245	62.034900	54.677293	43.889660
18300	61.881251	61.948060	54.513720	43.681390
18600	61.775209	61.923940	54.425922	43.586790
18900	61.747266	61.931700	54.386541	43.750780
19200	61.809428	61.938550	54.548393	43.713800
19500	61.746774	61.680040	54.366538	43.504940
19800	61.737605	62.006640	54.509239	43.714570
20100	61.705257	61.758050	54.495588	43.564030
20400	61.688014	61.859060	54.531207	43.732910
20700	61.820147	61.717560	54.511923	43.637400
21000	61.757625	61.831970	54.556578	43.646790

Start Time				
Elapsed Time	AN5D	AN6D	AN7D	AN8D
Seconds	C	C	C	C
13800	22.246320	11.888310	1.614103	1.735766
14100	22.157870	11.918360	1.504106	1.444393
14400	22.040050	11.761400	1.233536	1.285943
14700	21.877790	11.529620	1.335395	1.510065
15000	22.023540	11.651200	1.353506	1.357125
15300	22.180010	11.876950	1.421164	1.473418
15600	21.818130	11.384410	0.973490	0.883167
15900	21.762010	11.269930	1.042457	0.944341
16200	21.789680	11.445000	1.105233	0.986892
16500	21.745570	11.262090	1.076232	0.892458
16800	21.858100	11.540620	1.336021	1.256517
17100	21.926540	11.584420	1.300913	1.273278
17400	21.830580	11.586430	1.306090	1.210634
17700	21.829180	11.465670	1.230992	1.180423
18000	21.652080	11.245560	1.035985	0.982035
18300	21.791520	11.477300	1.225412	1.188417
18600	21.667130	11.170400	1.033978	0.963488
18900	21.778030	11.505660	1.350963	1.303958
19200	21.669310	11.171790	1.169232	1.087382
19500	21.849810	11.362300	1.336486	1.295833
19800	21.858880	11.320910	1.298821	1.095528
20100	21.802700	11.280310	1.171496	1.020207
20400	21.791080	11.424080	1.211951	1.125815
20700	21.766050	11.395330	1.046875	1.090300
21000	21.623620	11.243830	1.053091	1.058510

Start Time				
Elapsed Time	AN1D	AN2D	AN3D	AN4D
Seconds	C	C	C	C
21300	61.752878	61.633930	54.348954	43.567450
21600	61.716031	61.719380	54.362112	43.504600
21900	61.741479	61.950390	54.556312	43.788190
22200	61.744069	61.819170	54.485756	43.742590
22500	61.805966	61.821070	54.570340	43.710690
22800	61.752557	61.800010	54.446734	43.751080
23100	61.679467	61.775940	54.384988	43.735160
23400	61.789820	61.816520	54.496248	43.796410
23700	61.957382	61.832300	54.502960	43.743780
24000	61.683550	61.706590	54.524701	43.779950
24300	61.758644	61.909860	54.507591	43.857670
24600	61.756829	61.792850	54.353453	43.762160
24900	61.720132	61.787400	54.309081	43.721320
25200	61.578245	61.577040	54.305678	43.645770
25500	61.815815	61.869050	54.545384	43.783750
25800	61.674835	61.901880	54.327628	43.794180
26100	61.613127	61.503710	54.352130	43.644580
26400	61.667935	61.844380	54.257431	43.677930
26700	61.656270	61.533960	54.405123	43.632690
27000	61.805777	61.626760	54.414425	43.523700
27300	61.621692	61.801580	54.198257	43.574290
27600	61.672549	61.805140	54.403706	43.738350

Start Time				
Elapsed Time	AN5D	AN6D	AN7D	AN8D
Seconds	C	C	C	C
21300	21.875580	11.693980	1.475570	1.333667
21600	21.868000	11.527040	1.248563	1.224279
21900	21.718500	11.184330	0.966221	1.017070
22200	21.801040	11.396140	1.218888	1.110600
22500	21.714310	11.348250	1.086827	1.126610
22800	21.824840	11.326010	1.065437	0.993763
23100	21.892120	11.576350	1.259514	1.166002
23400	21.878720	11.450800	1.126609	1.030334
23700	21.866860	11.291690	1.053433	0.993915
24000	21.893130	11.542180	1.223097	1.194503
24300	21.978460	11.566820	1.097693	1.085997
24600	22.183290	11.880700	1.538748	1.383557
24900	22.322560	12.015080	1.707397	1.678296
25200	22.358600	12.154580	1.721494	1.820661
25500	22.187540	11.917490	1.694439	1.514389
25800	22.294640	11.892300	1.653200	1.538599
26100	22.131190	11.861610	1.535555	1.671936
26400	22.391130	12.072490	1.807410	1.705851
26700	22.111490	11.856090	1.629082	1.645221
27000	22.297950	11.911660	1.753617	1.647628
27300	22.266020	12.012250	1.849640	1.819377
27600	22.063570	11.894050	1.722989	1.658236

Appendix B: FORTRAN Code

```
module variables
integer,parameter::n=101
integer,parameter::m=101
integer iter,maxit,it
real(8),dimension(n,m)::T,Told
real(8)::dx,dy,k,e,lx,dt,Tc,Th,ly
real(8)::cpf,cps,cp,ro,Am
real(8)::alfa,T_m,sum,RR,R1,R,h1,h2
real(8),dimension(n,m)::a1,b1,c1,d1,a2,b2,c2,d2,error,xco
or,ycoor,d,b
end module variables
program home

use variables
maxit=6000
Th=334.15
Tc=274.15
dt=0.1
lx=0.125
ly=0.051
e=0.313
ro=598.44
k=0.28
cp=1000
alfa=k/(ro*cp)
dx=lx/(n-1)
dy=ly/(m-1)
time=0

do i=1,n
 do j=1,m

Told(i,j)=300

enddo
 enddo

 do i=1,n
  do j=1,m

xcoor(i,j)=(i-1)*dx
ycoor(i,j)=(j-1)*dy

enddo
 enddo

 do

 do i=1,n-1
```

```
  do j=1,m-1

error(i,j)=abs(T(i,j)-Told(i,j))
enddo
   enddo

T_m=maxval(error)

if (T_m < 0.0000001) exit

time=time+dt

call internal_coef

call boundary_coef


do iter=1,maxit

do i=1,n
 T(i,1)=274.15
end do

do i=1,n
 T(i,m)=334.15
end do

!call solver(T)

maxitT=1
call GAUSS_SEIDEL(T,maxitT)

 do i=1,n
 T(i,1)=274.15
end do

do i=1,n
 T(i,m)=334.15
end do

call residual

if(R<0.000001) exit

enddo

do i=1,n
   do j=1,m

Told(i,j)=T(i,j)
```

```
 enddo
    enddo

enddo

call exact ()

call print


end program home

subroutine internal_coef
use variables

h1=alfa*dt/2*dx**2
h2=alfa*dt/2*dy**2

    do i=2,n-1

     do j=2,m-1

a1(i,j)=-h1

!b1(i,j)=(2*h1)+1

c1(i,j)=-h1

!d1(i,j)=h2*Told(i,j-1)+(1-2*h2)*Told(i,j)+h2*Told(i,j+1)

b(i,j)=2*h1+2*h2+1

d(i,j)=h2*Told(i,j-1)+(1-2*h2-
2*h1)*Told(i,j)+h2*Told(i,j+1)   &
&      +h1*Told(i-1,j)+h1*Told(i+1,j)

a2(i,j)=-h2

!b2(i,j)=2*h2+1

c2(i,j)=-h2


!d2(i,j)=h1*Told(i-1,j)+(1-2*h1)*Told(i,j)+h1*Told(i+1,j)

   enddo
      enddo

  end subroutine internal_coef
```

```
  subroutine boundary_coef

    use variables

    i=1
    do j=1,m


!**********************westboundary*****************
    a1(i,j)=0
    !b1(i,j)=1
    b(i,j)=1
    c1(i,j)=-1
    !d2(i,j)=0
    d(i,j)=0

    enddo

    i=n
    do j=1,m

!**********************eastboundar******************
    a1(i,j)=-1
    !b1(i,j)=1
    b(i,j)=1
    c1(i,j)=0
    !d2(i,j)=0
    d(i,j)=0

    enddo

    j=1
    do i=1,n

!******************southboundary**********************

    a2(i,j)=0
    !b2(i,j)=1
    !b1(i,j)=1
    b(i,j)=1
    c2(i,j)=0
    !d1(i,j)=Tc
    d(i,j)=Tc

    enddo


    j=m
    do i=1,n
```

```
    !d1(i,j)=Th
!************************northboundary*****************
    a2(i,j)=0
    !b2(i,j)=1
    !b1(i,j)=1
    b(i,j)=1
    c2(i,j)=0
    d(i,j)=Th

    enddo

      end subroutine boundary_coef

SUBROUTINE GAUSS_SEIDEL(X,maxitT)
USE variables
REAL(8),DIMENSION(n,m) :: X
integer :: maxitT
maxitT=1
DO it=1,MAXITT
DO j=2,M-1
DO i=2,N-1


X(i,j)=(h1*X(i-1,j)+h1*X(i+1,j)+h2*X(i,j-1) &
&       +h2*X(i,j+1)+d(i,j))/b(i,j)
END DO
END DO
END DO
END SUBROUTINE GAUSS_SEIDEL


subroutine residual

use variables

open(7,file='out5.txt')

do i=2,n-1
 do j=2,m-1

 sum=0
 RR=0

 R1=h1*T(i-1,j)+h1*T(i+1,j)+h2*T(i,j-1) &

 &  +h2*T(i,j+1)+d(i,j)-b(i,j)*T(i,j)

 sum=sum+abs(R1)

 RR=RR+abs((b(i,j))*Told(i,j))
```

```
  enddo
 enddo

 R=sum/RR

 write(7,*)iter,R

 end subroutine residual

subroutine print

use variables

open(2,file='out1.txt')
write(2,*) 'zone i=',n,'j=',m,'f=point'


do i=1,n
do j=1,m

write(2,*) xcoor(i,j),ycoor(i,j),T(i,j)

enddo
  enddo

end subroutine print


subroutine exact ()
use variables

do j=1,m
i=1
T(i,j)=T(i+1,j)

enddo

do j=1,m
i=n

T(i,j)=T(i-1,j)

enddo

do i=1,n
j=1
T(i,j)=Tc
enddo

do i=1,n
j=m
```

```
T(i,j)=Th
enddo

end subroutine exact
```